MLM-3424
UC-4 and 22

MLM--3424

DE87 010638

Mound Activities in Chemical and Physical Research: July-December 1986

Issued: April 22, 1987

MOUND
Miamisburg, Ohio 45342

operated by
MONSANTO RESEARCH CORPORATION
a subsidiary of Monsanto Company

for the
U. S. DEPARTMENT OF ENERGY

Contract No. DE-AC04-76-DP00053

Foreword

This report is issued semiannually by Mound. These reports are not intended to constitute publication in any sense of the word. Final results either will be submitted for publication in regular professional journals or will be published in the form of MLM topical reports.

Previous reports in this series are:

MLM-3072	MLM-3258
MLM-3125	MLM-3305
MLM-3150	MLM-3347
MLM-3195	MLM-3389

MLM--3424
(DE87010638)
CONF-870610--1

Mound activities in chemical and physical research: July-December 1986

Little, J.B.

22 Apr 1987

Monsanto Research Corp., Miamisburg, OH (USA).
Mound

Contents

I. Low Temperature Research

Low Temperature Studies

G. T. McConville

A collaboration in low temperature thermometry between the metrology laboratories at Leiden, The Netherlands, and Turin, Italy, has resulted in a new set of ^{3}He virial coefficients and a comparison of the second virials calculated from the helium potential function developed at Mound with the data from both ^{3}He and ^{4}He. The collaboration produced two manuscripts to be published in the journal Metrologia. This work was done because of the proposed extension of the international practical temperature scale below the present low temperature limit of 13.81 K. Several scales have been proposed to go to lower temperatures based on the velocity of sound, magnetic moments, thermal noise, and the gas thermometer. At present, the gas thermometer is the leading contender between 24.55 and 4.2 K, the triple point of neon and the normal boiling point of ^{4}He, respectively. Below 4.2 K, the leading contenders are the vapor pressure of ^{4}He down to 2.2 K and the vapor pressure of ^{3}He down to 0.5 K. Realization of this proposed scale between 0.5 and 24.55 K would require three thermometric experimental setups.

Work on the ^{3}He virials was aimed at producing a scale that could cover the above temperature range. The second virial coefficient represents the largest correction in low temperature gas thermometry. Before the work of K. Berry in the 1970's [1], the uncertainty in the ^{4}He second virial represented the limiting uncertainty in low temperature gas thermometry. Berry measured one absolute isotherm at 20.27 K. He then made seven temperature determinations between 2.6 and 27.1 K relative to the absolute isotherm.

In Figure I-1, Berry's data are compared to three potential function calculations of the ^{4}He second virial. The traditional fitting function for the low temperature second virial is A + B/T, which to the accuracy of Berry's measurements is not quite right. Thus, Berry added a third term and fitted the data to $B(T) = 17.19 - 396.2T^{-1} - 48T^{-2}$ (cm^3/mole). It can be seen from the figure that the HFDHE2 function developed by Aziz, Nain, Carley, Taylor, and McConville [2] lies above the experimental error bars at temperatures below 5 K. This discrepancy led McConville [3] to modify the form of the HFDHE2 to fit the low temperature second virial data of Berry. The modification involved adding a βr^2 form to the repulsive exponential part of the function. The form is given in previous reports [4,5], and the value of $\beta = 0.01$ was determined to produce a desired fit to the data at 20.27 and 4.21 K. Subsequently, a mistake was found in the derivative of the potential function used in calculating the phase shifts. Correcting the derivative required changing β to 0.0099 to maintain the fit to the Berry data. This function is designated as HFDHE3 in Figure I-1.

A second, more complicated form of the helium potential function, the HFIMD (Hartree-Fock + intra-atomic correlation + model disperson), has been given by Feltgren et al. [6]. The main difference between the HFIMD and the HFD form is that the latter has the same damping term for all of the multipole attractive terms, whereas the former has a different damping term for each

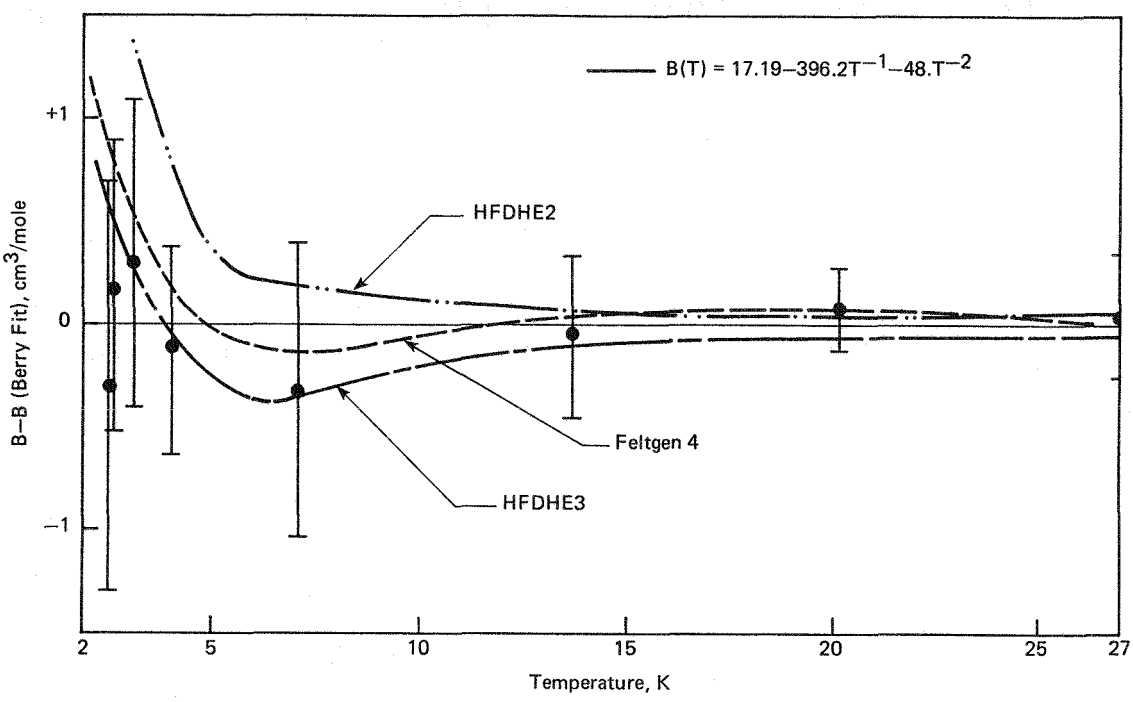

FIGURE I-1 - Comparison of potential function calculations to fit of Berry ^{4}He second virial data.

multipole form. The forms of the functions and a table of the constants used in the functions will be given later. The unknown constants in the HFIMD function were determined by inverting scattering data for both ^{3}He and ^{4}He. It was found that the low temperature ^{4}He second virial data were not well described with these constants [3]. Feltgen then used just his ^{4}He data to determine the constants and calculated the second virial in this case [7]. The curve in Figure I-1 labeled Feltgen 4 shows this calculation. All of the calculated curves in Figure I-1 turn up with respect to the data at low temperature.

Figure I-2 results from taking the Berry data and the above calculations and plotting them as a difference from the HFDHE3 calculation. Added to this figure are a data fit by Steur et al. [8] and two calculations by the present author to attempt to reproduce the Feltgen 4 calculation. The details of the calculations will follow. The data fit of Steur et al. is based on the surface fit program of Gugan [9] that determines second and third virials from isotherms. The data used in the fit were those of Berry and those of Kemp et al. [10] up to 84 K. When the Berry data are plotted with respect to a difference from the HFDHE3 calculation, only the lowest temperature experimental point differs by more than 0.3 cm^3/mole from the calculation. The lowest temperature point is within the experimental error bar. This point clearly influences the Steur fit below 5 K. Figures I-1 and I-2 show how the same data can be fitted to quite different functions with nearly the same precision, but with the big differences coming near the end of the region being fitted.

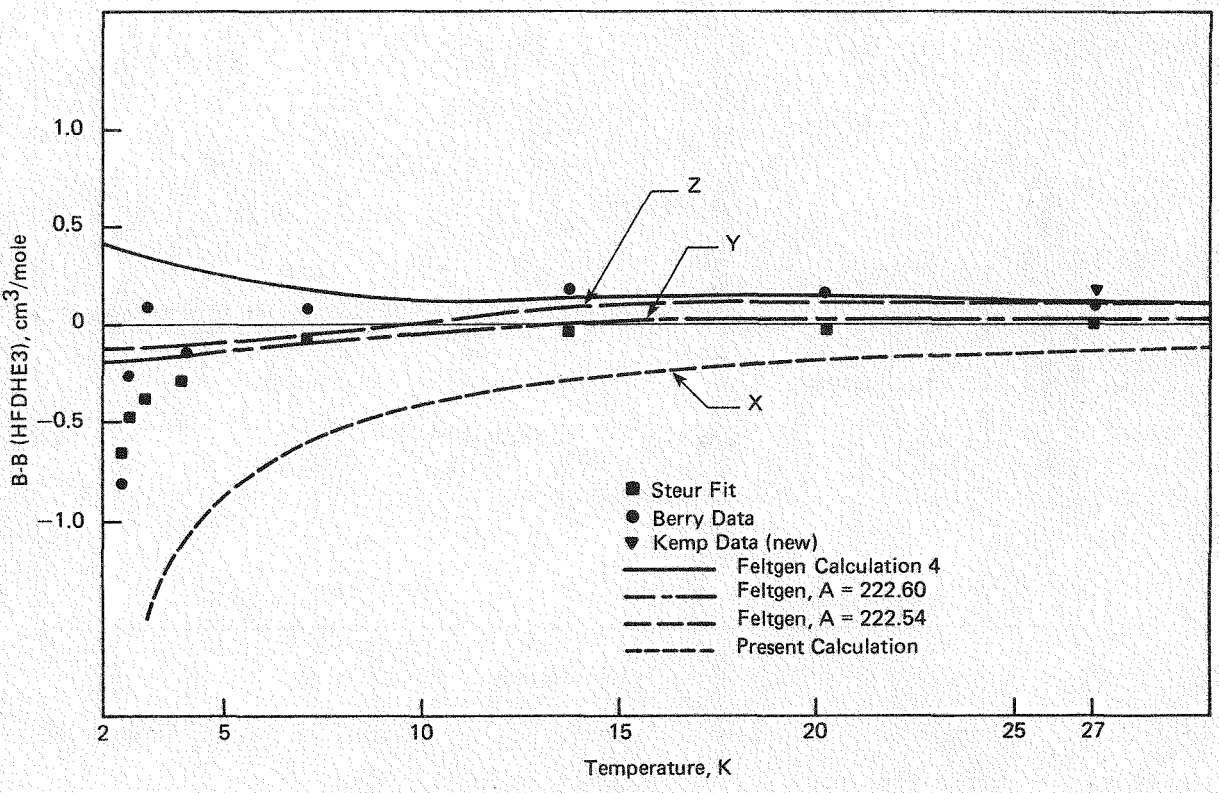

FIGURE I-2 - Comparison of Berry ^{4}He data and several versions of the HFIMD potential to the HFDHE3 potential calculation. X, Y, and Z explained in text.

A reanalysis of the Kemp et al. data at 27.01, 43.73, 54.33, 84.85, and 172 K in which B(T) is increased about 0.1 cm³/mole at 43 and 84 K is to be published soon [11]. These revised data and the data of Berry are compared with the HFDHE calculation over an extended temperature range in Figure I-3. The original Berry fit and the Steur fit are also shown. The data point at 273 K labeled Guildner appears in Guildner's gas thermometer article [12], but it is the unpublished work of M. Waxman. The error bar originally assigned to this point was 0.02 cm³/mole. A private communication from Aziz [13] indicated the error bar should be closer to 0.05 cm³/mole, which would allow for consistency between the virial data and viscosity data near room temperature. The HFDHE3 calculation would appear to represent the ^{4}He second virial data between 300 and 2.7 K well.

Returning to Figure I-2, consider the difference between the Feltgen 4 curves as calculated by Feltgen and the present calculations. In comparison to the HFD form of Ahlrichs et al. [14], the HFIMD is the more complex. Adding a second term to the repulsive exponent in the form of βr^2 to the Alhrichs HFD gives:

$$V = Ae^{-\alpha r - \beta r^2} + \sum_{n=1}^{3} \frac{C_{2(2+n)}}{r^{2(2+n)}} f(r) \qquad (1)$$

where the damping function, f(r), is given by:

$$F(r) = \exp - \left(\frac{Dr_m}{r} - 1 \right)^2 \qquad (2)$$

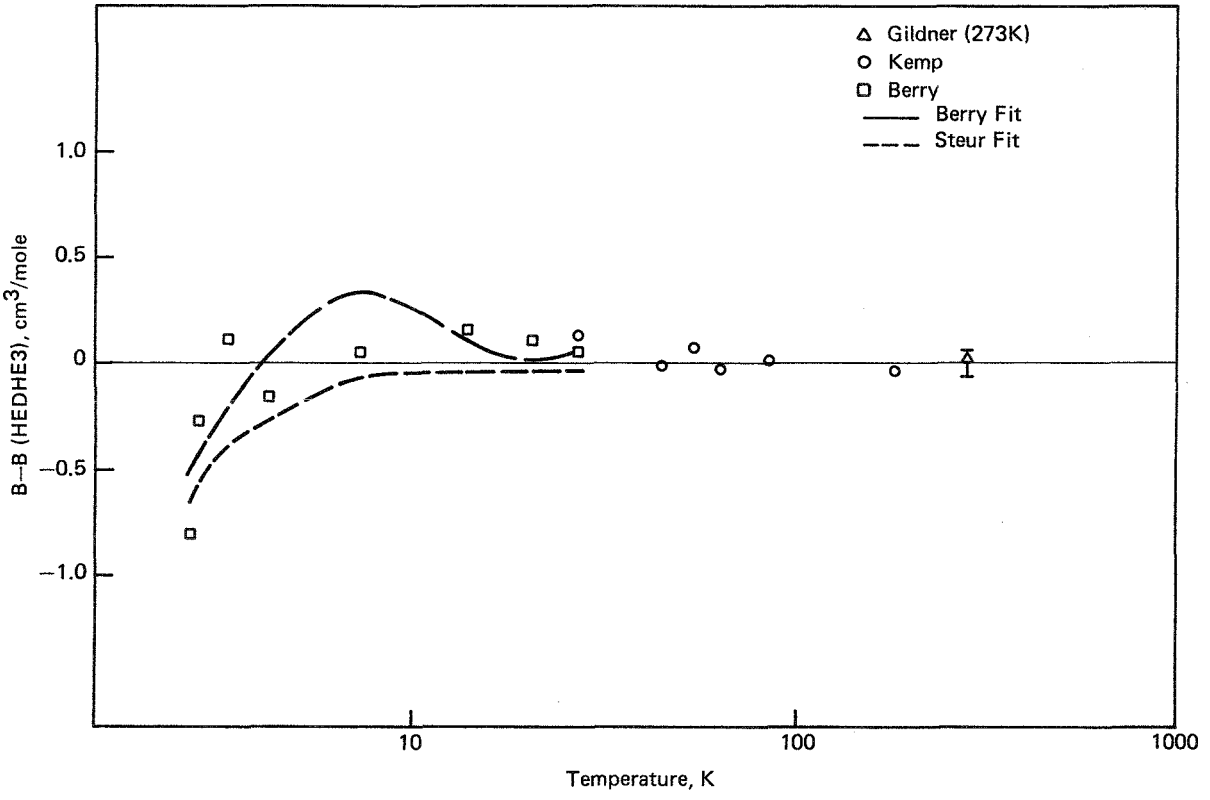

FIGURE I-3 - Comparison of Berry data fit and Steur data fit to data shown and the HFDHE3 potential calculation over an extended temperature range.

The addition of β allows β and D to be variable parameters through which the well depth can be changed without modifying the higher repulsive wall, thus maintaining the high temperature properties of the HFDHE2. A value of β = 0.0099 increases the well depth from 10.80 to 10.91 K.

The form of the HFIMD potential is nearly that of Equation (1), but the sum of attractive terms is given by n = 6 to 18, including odd terms, rather than 2(2+n). The odd terms arise from third order perturbation theory. The terms for n = 9 and 11 are zero. In the HFIMD there is an additional small repulsive term, Be^{-br}, to account for correlation among the electrons. The damping term is a modified incomplete gamma function derived from theory [4], and it depends on n in a complex way. Thus, the HFIMD form is:

$$V = Ae^{-\alpha r - \beta r^2} + Be^{-br} + \sum_{n=6}^{18} \frac{C_n}{r^n} f_n(r) \qquad (3)$$

where the damping function, a function of r, is:

$$fn^{(r)} = P(\alpha r,\nu)^2 + (a\ \alpha\ r)^m \exp(-1.4\ \alpha r) \qquad (4)$$

and $P(\alpha r,\nu)$ is the incomplete gamma function:

$$P(\alpha r,\nu) = \int_o^{\alpha r} e^{-t}\, t^{\nu-1} dt \qquad (5)$$

The quantity αr is given in Reference 6 as:

$$\alpha r = 8.5\ (1 + a_2 x) \qquad (6)$$

where $x = r/r_D$ and $r_D = 1.64$ Å. The parameters as given in Reference 6 are given in Table I-1. In this potential function, the two undetermined parameters, B and a_2, are determined by just the ^{4}He scattering data giving B as 24.4 meV and a_2 as 1.455. With these parameters, it was not possible to reproduce Feltgen's 4 calculations shown in Figures I-1 and I-2. The present calculation is shown in Figure I-2 as X and is low at all temperatures shown to 1 cm³/mole at 2 K. In reply to a question about the constants Feltgen actually used in the calculation, he returned all the numbers to eight places. There were two significant differences: A became 222.54 rather than 222.6 meV (Z and Y in Figure I-2) and αr became $8.5(1+a_2' r)$ rather than $8.5(1+a_2 x)$ where $a_2/r_D \neq a_2'$. a_2' was used in Feltgen's calculation. If A = 222.54 is used, the energy as a function of r table for the HFIMD can be reproduced, but Feltgen 4 values of the second virial cannot. If A = 222.54 and B = 28.4, the curve labeled Y in Figure I-2 is obtained. If A = 222.60 and B is decreased to 24.4, the value used in Feltgen 4, the curve labeled Z in Figure I-2 is obtained. This curve agrees with Feltgen 4 down to 15 K, with a divergence up to 0.5 cm³/mole at 2 K. This divergence at the moment is unexplained. Feltgen et al. used formula 6.4-11 from Hirschfelder, Curtiss, and Bird [15] to calculate the second virial. This formula contains the derivative of the phase shift with respect to energy. An integration by parts of the last term converts the derivative back to the phase shift. This difference in calculational technique may account for the low temperature differences. Mound calculations from the HFDHE3 and the HFIMD were done in the same way. On the basis of the present calculations, it appears that the HFIMD form (curve Z) describes Berry's ^{4}He data better than the HFDHE3 does.

Now look at the ^{3}He measurements of the second virial. Use of ^{3}He in the gas thermometer could extend the temperature range from the present low with ^{4}He at 2.6 K to below 1.0 K. The practical limit with a standard gas thermometer will be about 1.2 K. Until recently, there were no second virial measurements on ^{3}He of the quality of those by Berry on ^{4}He. Then Matacotta of IMGC, McConville of Mound, and Steur and Durieux of KOL [16] obtained a relative set of ^{3}He virials between 20.3 and 1.5 K. These are relative to the Berry ^{4}He virial at 20.3 K, assuming the ^{3}He and ^{4}He second virials can be described by the same potential function. These data are displayed in Figure I-4 as a difference from B calculated with the HFDHE3 potential function. The data of Cameron and Seidel [17] extending below 1.5 K were taken from a novel gas cell in which the density was directly measured using a superconducting niobium cavity. Two different analyses of the data of Keller [18,19] are given. The HFDHE3 calculation appears to be the most consistent with the recent data taken at KOL, Leiden.

The KOL data were not corrected for any effect of the third virial because the data, although taken at four densities, were not taken at high enough densities to extract both second and third virials simultaneously. Thus, the difference between the data fit and the HFDHE3

Table I-1 - POTENTIAL PARAMETERS[a]

From Theory	HFDHE3	HFDIMD 4
A		2.58289×10^6
α	4.48	3.8073
β		0.12955
b		4.54
C_6	-1.012344×10^4	-1.0107×10^4
C_8	-2.76109×10^4	-2.7722×10^4
C_{10}	-1.01786×10^5	-9.8370×10^4
C_{11}		1.2716×10^4
C_{12}		-4.9858×10^5
C_{13}		1.2079×10^5
C_{14}		-3.3811×10^6
C_{15}		1.1278×10^6
C_{16}		-3.0249×10^7
C_{17}		1.2647×10^7
C_{18}		-3.3428×10^8
Adjustable		
β	0.0099	
Dr_m	3.7161	
B		2.8311×10^5
a_2		1.455
Derived		
E/K	10.912	10.94
r_m	2.9652	2.964
r_o	2.6372	2.638

[a]Units: Kelvins, angstroms.

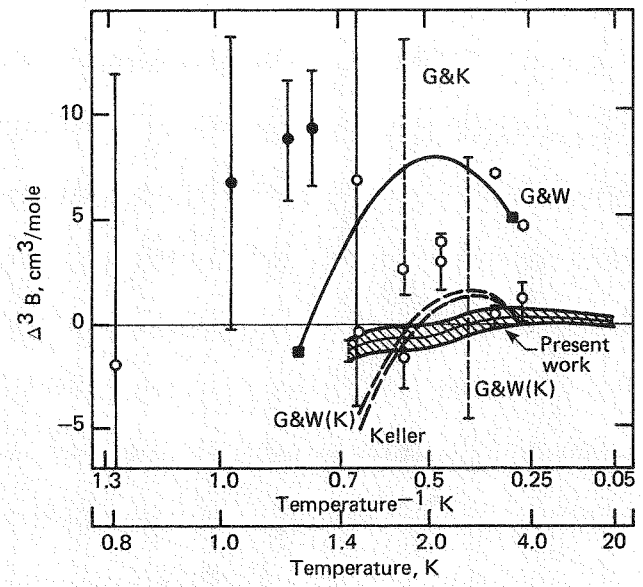

FIGURE I-4 - All the ^{3}He second virial data are compared to the HFDHE3 potential calculation.

calculation has an effect of the third virial in it. The data fit, shown on an expanded scale in Figure I-5, is compared to the HFDHE3 calculation. The average deviation of the data from the fit at each measured temperature is given by an open circle. The solid vertical line represents the temperature uncertainty in a gas thermometer operating at a density of 309.5 mole/m^3 of 0.5 mK caused by a deviation ΔB shown in the figure. In Figure I-6, the HFIMD calculations for cases Y and Z fall lower than the HFDHE3 calculation but have the same general shape. The difference in the calculations arises in the difference in the shape of the bottom of the potential well of the two different functions. The difference in the curves probably

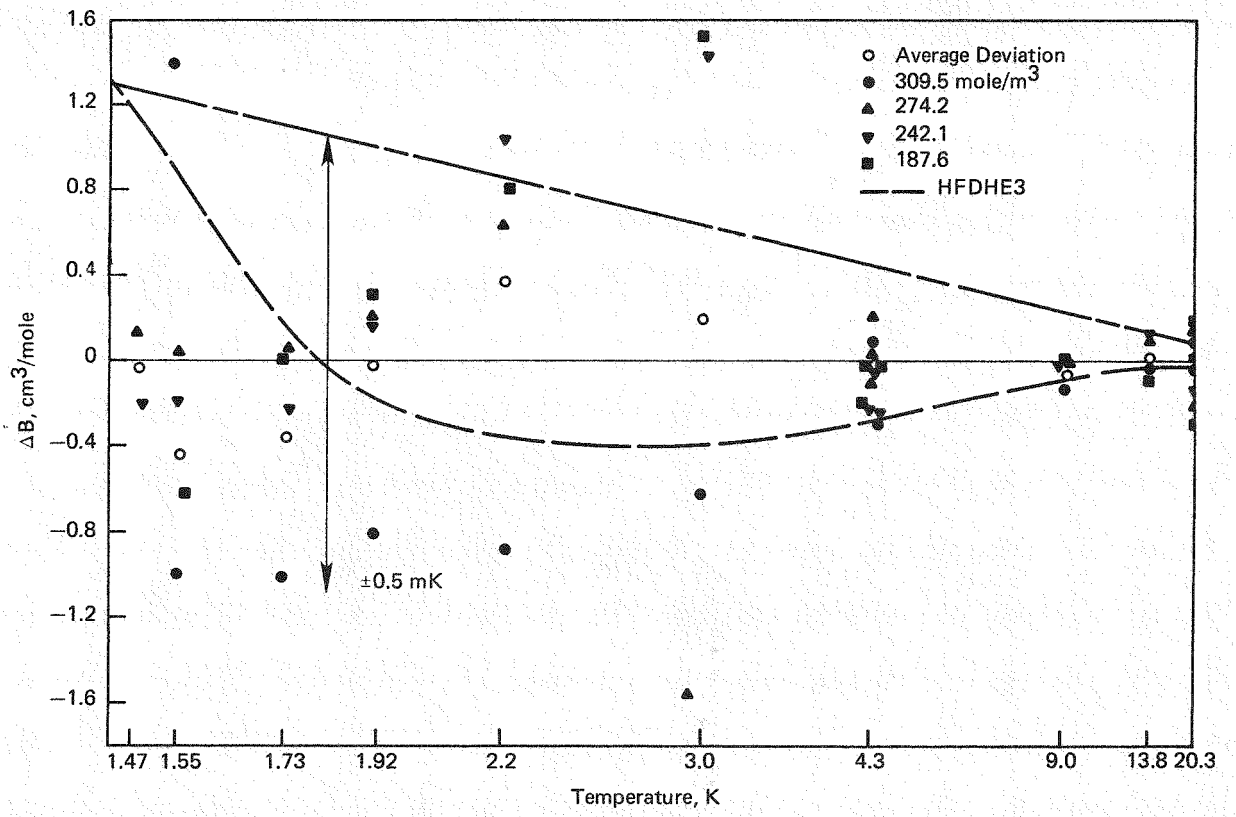

FIGURE I-5 - Comparison of HFDHE3 potential calculation and the Leiden data to the data fit: $B = 16.69 - 336.98/T + 91.04/T^2 - 13.82/T^3$.

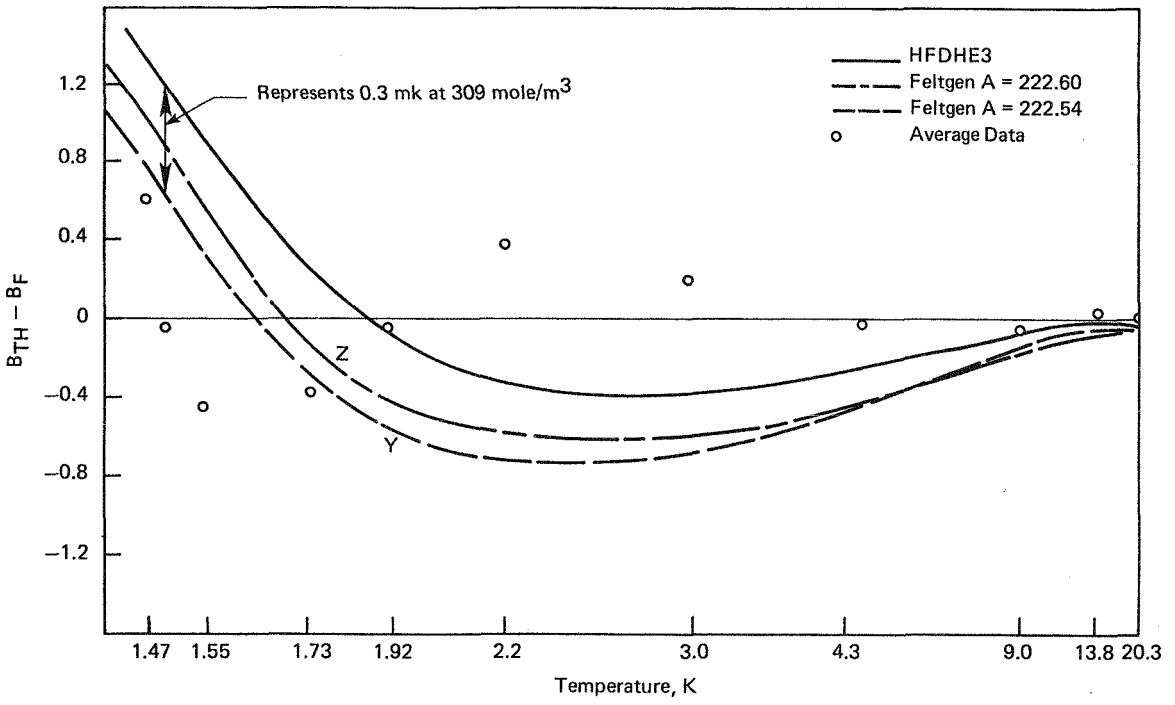

FIGURE I-6 - Comparison of HFDHE3 and versions Y and Z of HFIMD to the data fit given in Figure I-5.

represents a real uncertainty in the potential function resulting from the choice of damping functions.

The shape of the difference between the data fit and the potential calculation is similar to that of the inverse of the temperature dependence of the third virial, C(T), for ^{4}He. The form determined by the Steur surface fit for ^{4}He is $C(T) = 93 + 4542/T - 1.95 \times 10^6/T^7$ cm³/mole. The differences, ΔB [B(measured) - B(calculated)], are given as a function of temperature in Table I-2. The values of C in Table I-2 were then fit to $C(T) = C_1 + C_2/T + C_3/T^n$ where C_1 was constrained to be the same as that for ^{4}He. The best least squares fit was obtained for $C_1 = 93$, $C_2 = 2971$, and $C_3 = -5.74 \times 10^4$ with $n = 5$. Then $\Delta B = C(T)\ (N/V)$ was added to the calculated B to obtain a corrected measured virial at each point. These points relative to their best least squares fit are shown in Figure I-7. Correcting for the third virial reduced the scatter in the data in Figure I-5 by about 5%. The dashed curve in Figure I-7 represents the calculated second virial, which describes the fit to the data to within 0.2 cm³/mole above 1.5 K.

The comparisons shown in Figures I-2, I-3, and I-7 indicate that the calculated virial from the HFDHE3 can describe both the ^{4}He and the ^{3}He data to 0.2 cm³/mole between 1.5 and 300 K. The potential function, not the data, determines the mathematical form of the temperature dependence of the second virial. The comparison to the HFIMD indicates that the uncertainty in the second virial as a result of the potential form is less than 0.3 cm³/mole. Thus, it appears reasonable to suggest that the calculated temperature dependence for the second virial of ^{4}He and for ^{3}He be used to define the second virial correction for the interpolating gas thermometer.

Table I-2 - HFDHE3

Temperature (K)	B Virial Coefficient	$B_m - B_c$ (cm³/mole)	N/V	C (cm³/mole)²
20.39	0.410	0.074		239
4.32	-56.918	0.381		1233
20.42	0.435	-0.042		- 136
1.55	-165.348	-0.278		- 899
4.53	-53.633	0.217		702
1.47	-173.235	-0.995		-3219
4.40	-55.603	0.291		941
1.56	-164.802	-2.008	3.09052×10^{-4}	-6497
1.72	-151.045	-1.3335		-4320
1.91	-136.385	-0.715		-2313
4.37	-55.994	-0.024		- 77
9.01	-19.757	-0.016		- 52
13.84	-7.194	-0.084		- 271
20.26	0.302	-0.079		- 255
20.26	0.301	-0.108		- 399
4.28	-57.449	0.692		-2525
20.41	0.425	0.013		47
4.29	-57.425	0.160		583
1.51	-169.489	-1.151		-4235
1.57	-163.443	-1.007		-3674
1.74	-149.133	-0.167	2.74096×10^{-4}	- 609
1.92	-135.858	+0.408		1488
4.30	-57.120	0.533		1944
9.04	-19.608	0.121		441
13.86	-7.159	0.062		226
20.25	0.294	0.130		474
20.28	0.317	0.015		69
4.35	-56.331	0.268		1106
9.02	-19.705	0.116		479
13.84	-7.192	0.085		351
20.49	0.483	0.096		396
4.29	-57.424	0.268	2.42240×10^{-4}	1106
1.52	-168.594	-1.536		-6341
1.56	-164.558	-1.312		-5416
1.74	-149.149	-0.491		-2027
1.90	-137.710	0.490		2022
4.38	-55.869	0.012		49
20.27	0.308	-0.133		- 549
20.36	0.380	0.180		957
4.22	-58.559	0.268		1425
9.04	-19.633	0.122		649
13.85	-7.179	-0.124	1.88077×10^{-4}	- 659
20.37	0.394	0.073		388
1.47	-173.794	-0.696		-3700
1.55	-165.561	-1.819		-9671
1.72	-150.650	-0.330		-1756
1.92	-135.986	0.536		2850
4.26	-57.875	0.124		659
20.26	0.305	-0.301		-1600

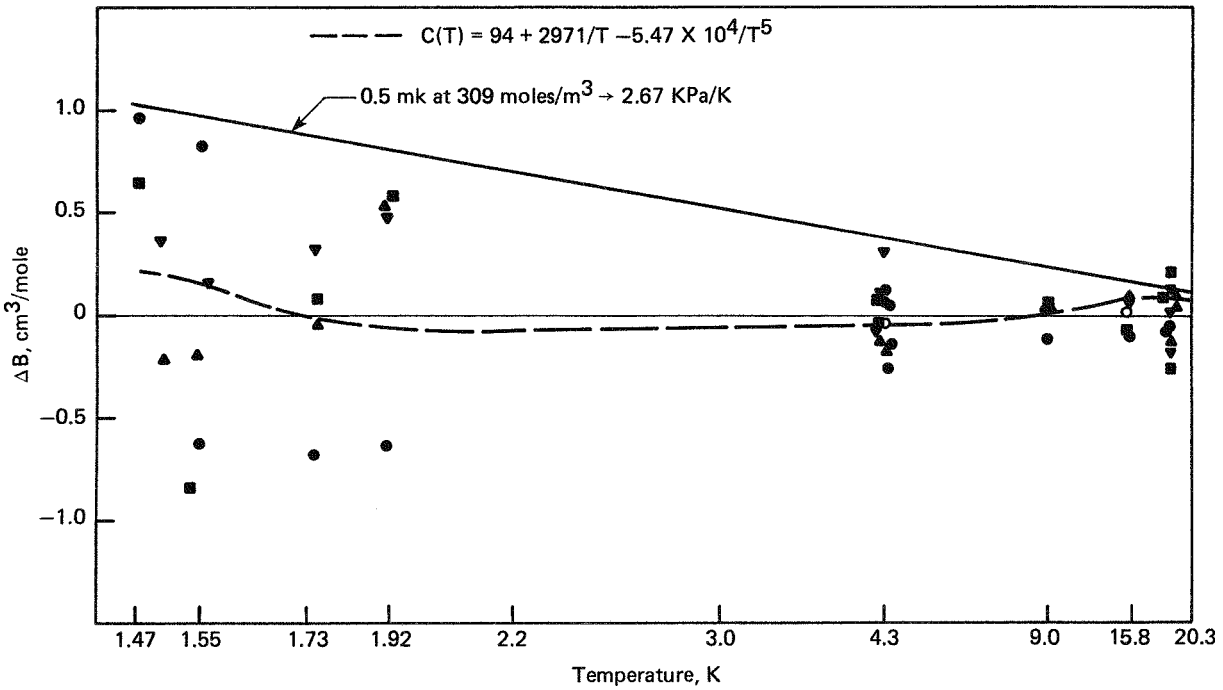

FIGURE I-7 - Comparison of HFDHE calculation and data after correction for effect of third virial, C(T).

II. Separation Research

Liquid Phase Thermal Diffusion

W. M. Rutherford

A. THERMAL DIFFUSION OF DEUTERATED BENZENES

Previous research has shown that isotopic thermal diffusion in liquids is dependent not only on mass differences, but also on differences in mass distribution between diffusing molecules. It was found, for instance, that isotopic thermal diffusion in substituted benzene systems is well represented by the equation:

$$\alpha_T = 1.973(m_1 - m_2)/(_1 + m_2) + 0.973(I_1 - I_2)/(I_1 + I_2) \quad (1)$$

where α_T is the isotopic thermal diffusion factor, m_1 and m_2 are molecular masses, and I_1 and I_2 are second moments about an axis perpendicular to the plane of the benzene ring [1].

In subsequent work [2], it was found that thermal diffusion among the several species of isotopically substituted carbon disulfide molecules is given by:

$$\alpha_T = 2.20(m_1 - m_2)/(m_1 + m_2) + 1.67(I_1 - I_2)/(I_1 + I_2) \quad (2)$$

Ma and Beyerlein published results of thermal diffusion measurements involving deuterium substitutions at various locations in methanol and benzene [3]. Significant effects of mass distribution were reported. Their measurements for benzene-benzene d_6 and benzene-benzene 1,4 d_2 were in reasonable agreement with Equation (1). The result for benzene-benzene 1,2 d_2, however, was anomalously low. Equation (1) predicts a value of 0.057 for the thermal diffusion factor of the benzene-benzene 1,2 d_2 pair, whereas the value reported by Ma and Beyerlein was 0.01.

As the result of preliminary work at this laboratory [4], a much higher value of 0.066 was found for the thermal diffusion factor of the benzene-benzene 1,2 d_2 pair, a result that is in considerably better agreement with Equation (1). Thus, it appeared likely that the Ma and Beyerlein measurement for the 1,2 d_2 system was in error.

A more thorough investigation of thermal diffusion in deuterated benzene systems has now been completed, and the results are included in this report. Measurements were completed for three systems: benzene-benzene d_6, benzene-benzene 1,4 d_2, benzene-benzene 1,2 d_2.

Two columns, 46 mm long with different hot to cold wall spacings, were used for these experiments. Binary mixtures were prepared from reagent grade benzene and isotopically substituted benzenes purchased from Cambridge Isotope Laboratories, Woburn, Massachusetts. Identity and purity of the compounds were verified by infrared and Raman spectroscopy and by nuclear magnetic resonance spectroscopy. The dideuterobenzene mixtures were 15% by volume of isotopically substituted material, and the perdeuterated benzene was 35% by volume.

Results of the measurements are given in Table II-1. This table includes a parameter F that was defined in previous work as an approximate measure of the ratio of the internal circulation rate in the column to that calculated theory. It is given by

Table II-1 - RESULTS OF THERMAL DIFFUSION EXPERIMENTS WITH DEUTERATED BENZENE MIXTURES

Compound	Column	Thermal Diffusion Factor	F
Benzene 1,4 d_2	A	0.061	1.09
	B	0.055	1.04
		0.061	1.04
	Average:	0.059 ± 0.003	
	Equation (1):	0.058	
Benzene 1,2 d_2	A	0.064	1.03
		0.063	1.05
	B	0.056	1.00
		0.057	1.03
	Average:	0.060 ± 0.003	
	Equation (1):	0.057	
Benzene d_6	A	0.179	1.02
		0.184	1.00
	B	0.156	0.94
		0.160	0.95
	Average:	0.170 ± 0.012	
	Equation (1):	0.178	

The average temperature for Column A was 68°C, and for Column B it was 61°C. The temperature differences were 68°C and 79°C, respectively. The hot to cold wall spacings were 255.9 and 318.6 μm.

$$F = (K_{exptl}/K_{theory})^{1/2} \quad (3)$$

where K_{exptl} is the experimental remixing coefficient and K_{theory} is the coefficient calculated from the theory of the thermal diffusion column. K_{exptl} is calculated from

$$K_{exptl} = HL/Y \quad (4)$$

where H is the observed initial transport coefficient, L is the length of the column, and Y = ln q, where q is the equilibrium separation factor. The departure of F from unity is a measure of the discrepancy between the observed column performance and that predicted from the theory of the thermal diffusion column.

Experimental thermal diffusion factors for all three systems agree quite closely with the predictions of Equation (1). The value obtained for the benzene-benzene d_6 pair is essentially identical to that obtained in earlier work. As predicted, the thermal diffusion factors of the two dideuterobenzene systems are nearly equal in spite of the considerable difference in symmetry of the two molecules. These results indicate that symmetry, per se, does not have a large influence on isotopic thermal diffusion. It seems that the distance of the mass

substitution from the center of the mass, as expressed in the second moment term of Equation (1), is the dominant effect of mass distribution within the molecule. Thus, differences in rotational inertia contribute significantly to the isotopic thermal diffusion effect in liquids.

B. SEPARATION OF SILICON ISOTOPES BY THERMAL DIFFUSION

It has been demonstrated that the isotopes of silicon can be separated by liquid phase thermal diffusion of organosilicon compounds. In previous experiments [5], the thermal diffusion factor for the ^{30}Si-^{28}Si pair in tetramethylsilane was found to be large enough to support a practical scale separation process, and the fluid was found to be chemically stable for extended periods at normal operating temperatures.

Additional progress was made toward demonstrating a practical process for ^{30}Si separation. The essential characteristics of optimum key weight cascades for various product enrichments were estimated by the method of de la Garza [6]. Subsequently, available equipment was reconditioned and assembled into a four-column experimental separation cascade that was later lengthened to nine columns.

If hydrogen isotopes are neglected, natural tetramethylsilane comprises 15 possible combinations of three silicon isotopes and two carbon isotopes. Of the 15, there are only seven that are present in any significant concentration (more than 0.01%). The normalized, seven-component composition of natural tetramethylsilane is given in Table II-2, along with the natural abundances of silicon and carbon isotopes.

Previous research has demonstrated that the effect of unit mass substitution on the thermal diffusion factor is strongly dependent on position within the molecule. Different equivalent masses for carbon and silicon isotopic substitutions can be assigned in theoretical calculations to accommodate this effect. Thus, based on the experimental work reported earlier [5], a single unit mass substitution at a carbon position in tetramethylsilane was found to be equivalent to a 1.2 unit mass substitution at a silicon position.

On the basis of these considerations, the properties of a series of optimum key weight cascades were estimated for product enrichments ranging from 22 to 88% ^{30}Si. The most significant property of these cascades is the dimensionless length required to reach a given product enrichment. This length, which is plotted in Figure II-1, appears to be readily achievable up to concentrations of approximately 75% ^{30}Si. (Y in Figure II-1 is defined as the logarithm of the equilibrium separation factor per unit mass.) Beyond about 75% it becomes increasingly necessary to make a difficult split between $^{30}Si(^{12}CH_4)_4$ and $^{29}Si(^{13}CH_4)(^{12}CH_4)_3$.

Experimental work on silicon isotope separation was started with a four-column system that was later extended to nine columns. The parameters of the several columns, which are connected in series, are given in Table II-3. The parameter H in Table II-3 is the initial transport rate of tetramethylsilane per unit mass difference.

By the usual criteria, the dimensionless length of the nine-column system is barely adequate to support production of

Table II-2 - SILICON AND CARBON ISOTOPIC ABUNDANCES IN TETRAMETHYLSILANE

Atom or Molecule	Abundance (%)
^{12}C	98.9
^{13}C	1.1
^{28}Si	92.21
^{29}Si	4.70
^{30}Si	3.09
$^{28}Si(^{12}CH_4)_4$	88.22
$^{28}Si(^{13}CH_4)(^{12}CH_4)_3$	3.92
$^{28}Si(^{13}CH_4)_2(^{12}CH_4)_2$	0.07
$^{29}Si(^{12}CH_4)_4$	4.50
$^{29}Si(^{13}CH_4)(^{12}CH_4)_3$	0.20
$^{30}Si(^{12}CH_4)_4$	2.96
$^{30}Si(^{13}CH_4)(^{12}CH_4)_3$	0.13

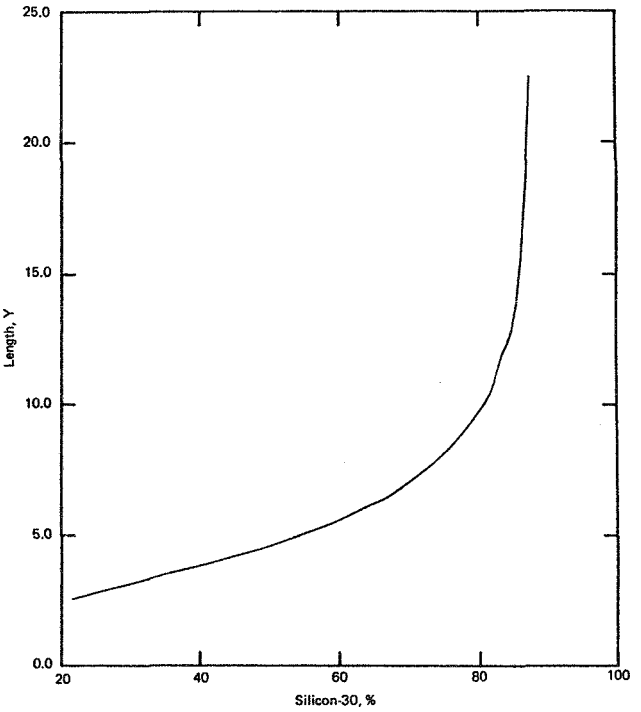

FIGURE II-1 - Dimensionless length of optimum key weight cascades for ^{30}Si separation.

Table II-3 - COLUMN PARAMETERS FOR THE TETRAMETHYLSILANE CASCADE

Column	Length (m)	Spacing (μm)	10^5H (g/s)	Y
1	1.13	305	7.02	0.15
2	1.14	305	7.02	0.15
3	1.17	254	3.76	0.32
4	1.17	254	3.76	0.32
5	1.16	254	3.76	0.32
6	1.14	254	3.76	0.32
7	0.61	254	3.76	0.17
8	0.76	254	3.76	0.21
9	0.76	254	3.76	0.21

^{30}Si at 20% enrichment; however, higher concentrations are clearly more desirable. Accordingly, withdrawal of product was deferred in order to allow the cascade to accumulate inventory and to allow the concentration to increase beyond 20%.

Figure II-2 is a plot of the transient behavior of the system as calculated from theory. Because of the discontinuous nature of the experimental operation, it is not possible to make a direct comparison with observed results during the early phases of the operation. A comparison can be made at later times, however, by shifting the time scale linearly so that the theoretical and observed end concentrations match at a suitable point. The first experimental point plotted in Figure II-2 was chosen as the match point. At that time concentrations had settled following extension of the system to nine columns, and there were no further interruptions in utility services. That day was found to be equivalent to 31.8 days in the theoretical calculation. The remaining experimental concentrations in Figure II-2, therefore, are plotted relative to day 31.8.

Progress of the ^{13}C concentration at the end of the cascade is also plotted as a function of time in Figure II-3. Again, the experimental data are plotted using 31.8 days as a reference point with respect to the theoretical calculation. Figure II-3 shows that the observed change in ^{13}C concentration is fairly well matched by the results of the calculation. This is a sensitive indicator of the accuracy of the assumed equivalent mass for a ^{13}C substitution in tetramethylsilane. It is apparent from Figure II-3 that the choice of 1.2 for equivalent mass is reasonably accurate.

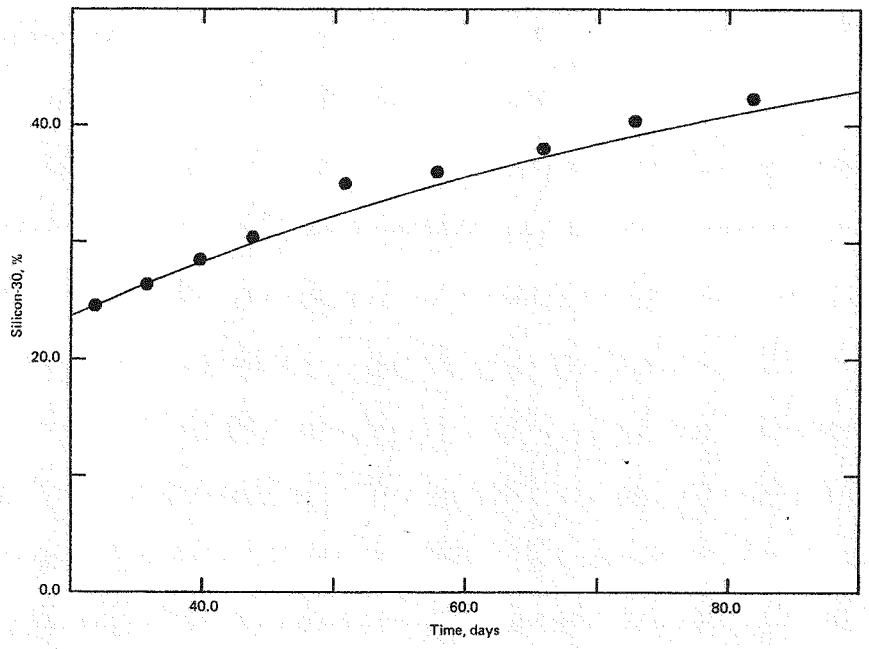

FIGURE II-2 - Separation of ^{30}Si in a nine-column thermal diffusion cascade. The solid line is calculated from theory, and the abscissa is the time from the theoretical calculation.

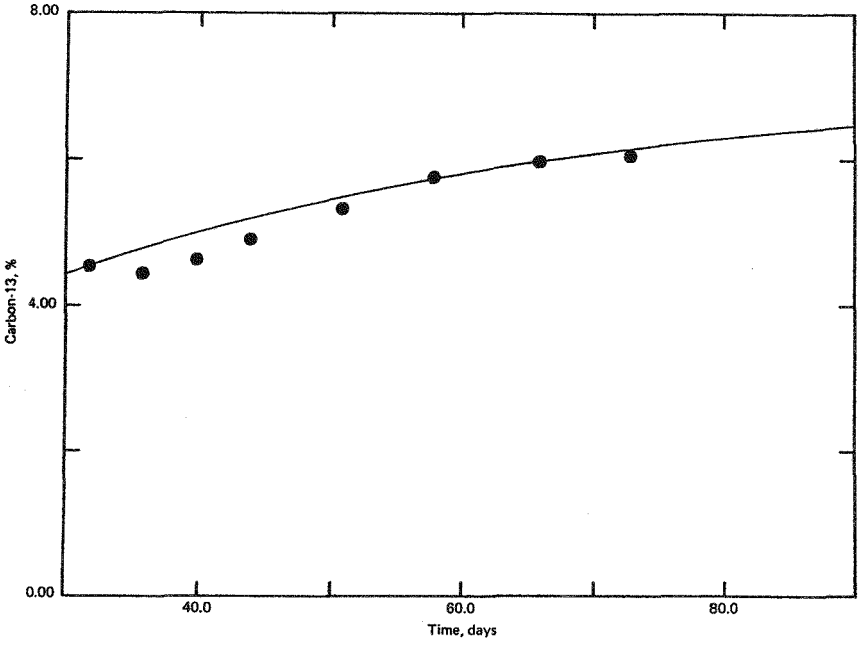

FIGURE II-3 - ^{13}C in the nine-column tetramethylsilane cascade. The solid line is calculated from theory, and the abscissa is the time from the theoretical calculation.

Calcium Chemical Exchange

B. E. Jepson and W. F. Evans

Investigations are continuing as part of the ongoing search for a practical chemical method of separating calcium isotopes. The identification and implementation of such a method promises the availability of comparatively inexpensive separated calcium isotopes for use as stable isotopic tracers. To date, work toward this goal has focused on two general approaches: ion exchange chromatography and liquid-liquid chemical exchange. A third method, "extraction" chromatography, will be added for investigation. As its name implies, extraction chromatography combines elements of both solvent extraction and chromatography. Hence, it may overcome some of the problems hindering the development of an economic process based on either liquid-liquid or chromatographic techniques.

Recent advances in areas such as extractants, chromatographic packings, and equipment have opened up new avenues to explore in seeking isotope separation systems. However, the inherent difficulty of calcium isotope ratio measurements has retarded progress in these new areas as it has in existing areas of exploration. Continued problems in obtaining accurate, precise, and timely isotope ratios have forced much of the work described below to remain incomplete. Efforts are still under way to reduce the problems, and the isotope ratio measurements which are in process will be presented in future reports of this series.

This report describes recent calcium column experiments and presents partial and preliminary data obtained for two previous column experiments. New

directions in liquid-liquid chemical exchange involving various liquid ion exchange reagents will be touched on. Also, the development of two different phase separation schemes for use in the determination of heterogeneous isotope exchange rates will be discussed.

COLUMN CHROMATOGRAPHY

Cryptand Screening Experiments

Heumann and Schiefer [7] have reported separation factors in the range of 1.0026 to 1.0057 for the $^{44}Ca/^{40}Ca$ pair in liquid-liquid systems using cryptand (2B,2,2). Characterization experiments are being performed with this and other cryptand ligands to continue assessing the potential of these types of macrocyclic compounds for calcium isotope separation. The end result of these experiments will be the determination of the magnitude and direction of the calcium isotope effects obtainable with cryptands bound to a resin phase.

Comparatively low fluid phase calcium concentrations are desired for isotope exchange column experiments since a high solid phase to fluid phase concentration ratio is needed in order to avoid excessively long theoretical plate heights. Hence, the behavior of the calcium breakthrough front for a system employing a cryptand resin and a dilute calcium fluid phase is an important consideration. To examine the nature of such a breakthrough, a 20-cm long column was packed with 5.5 cm³ of 222B resin (Kryptofix® 222B polymer*). The packing was washed with deionized water until the effluent from the column attained a pH of 4.8. Flame emission measurements (Buck Scientific Co. Model 200 AAS) indicated no detectable calcium, sodium, or potassium contamination in the effluent. The column was then washed with degassed 99:1 MeOH:H_2O (by volume). The calcium feed solution was 0.025 M $CaCl_2$ in 99:1 MeOH:H_2O (by volume) and was passed through the column under gravity flow. Periodically, aliquots of the effluent were removed and analyzed for calcium concentration by atomic absorption spectroscopy (propane/air flame, Buck Scientific Co. Model 200 AAS). The breakthrough profile is shown in Figure II-4. Resin expansion under these conditions was estimated to be approximately 0.9% (expansion from 5.50 to 5.55 cm³) with the introduction of calcium to the column. Following the breakthrough, the capacity of the column was verified by recovery and quantitation of the resin-bound calcium. The 222B resin calcium capacity was calculated to be 0.15 mmole/cm³. This information was used to design a 100-cm column experiment to measure precisely the isotopic separation factor for the $CaCl_2$/MeOH/H_2O-222B resin system (see Figure II-4).

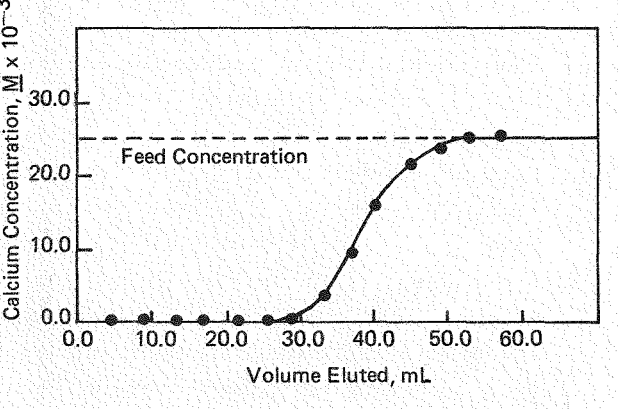

FIGURE II-4 - Calcium breakthrough profile from 222B Cryptand resin screening experiment.

*E. Merck product consisting of insoluble Kryptofix® 222B bound to Merrifield resin via an ether linkage.

Characterization of the calcium breakthrough was also accomplished for 221B cryptand resin (Kryptofix® 221B polymer*). The packing was washed with approximately 400 mL of deionized H_2O to remove sodium impurities present before preloading with lithium. During preloading, 0.15 M LiCl in MeOH was passed through the column under gravity flow until the lithium content in the effluent reached the constant feed value as monitored by flame emission. Lithium first appeared in the effluent after approximately 0.675 mmoles of lithium was fed to the column, and the breakthrough was complete after 0.825 mmoles had been added (Figure II-5). A 0.105 M $CaCl_2$-MeOH feed solution was passed through the column under gravity flow. Aliquots of the effluent were removed at 0.5 mL intervals and analyzed for calcium concentration by atomic absorption spectroscopy as above. The breakthrough curve in Figure II-5 indicates acceptable column capacity and band front shape for further work. An experiment will be performed with a 100-cm column to measure precisely the isotopic separation factor for this system.

Calcium Chloride - 222B Cryptand Resin Column Experiment

A standard glass chromatography column, 6.3-mm i.d. x 109 cm long, was filled with approximately 14 g of Kryptofix® 222B polymer (combined MC/B-Merck lot numbers 12L21, 12M02, and 12J04) as follows. The resin was slurried with a 49.1:50.9 MeOH:H_2O (by volume) solution and added to the column through a packing reservoir. The settling rate under gravity flow was less than 1.5 cm^3/min. Particle size fractionation occurred during the settling process, and a considerable quantity of "fines" was present. The column was backwashed with deionized H_2O at a rate of 2.0 mL/min to completely fluidize the resin bed. After the resin settled, this process was repeated three times, with the "fines"

*E. Merck product consisting of insoluble Kryptofix® 221B bound to Merrifield resin via an ether linkage.

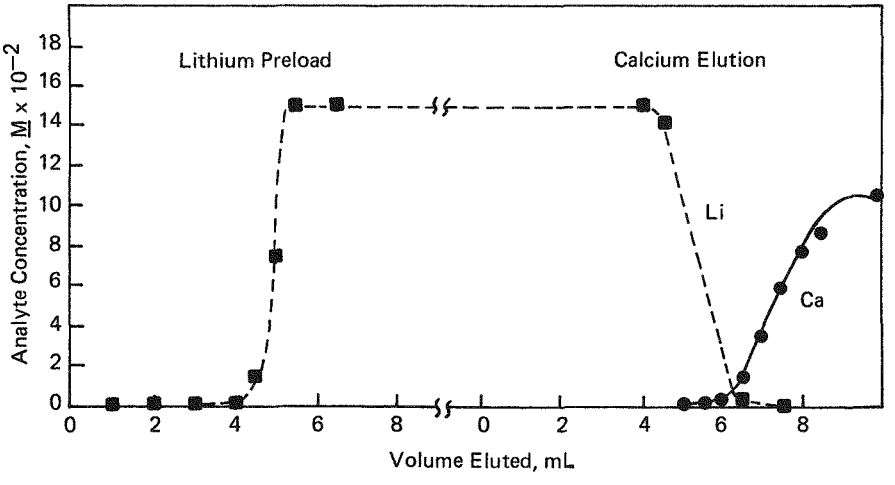

FIGURE II-5 - Lithium and calcium profiles from 221B Cryptand screening experiment.

pumped off as waste. The column was washed with deionized H_2O, and the effluent was monitored for sodium contamination by flame emission. Approximately 400 mL of water was required to remove the sodium contamination from the column. The column wash solution was switched to a $MeOH/H_2O$ gradient by increasing the methanol content in steps of approximately 25 vol % to a final composition of 98.9:1.1 $MeOH:H_2O$. These wash solutions were degassed before use. The column was backwashed and fluidized as needed during the wash process to correct the low flow rates caused by resin compaction. The resin bed depth was 99.7 ± 0.1 cm at the start of the experiment.

A feed solution (500 mL) consisting of 0.027 M $CaCl_2$ in 99:1 $MeOH:H_2O$ (by volume) was prepared. K^+-free CaO was added to deionized H_2O containing the stoichiometric quantity of HCl required for reaction with the CaO. Methanol (Mallinckrodt Anhydrous AR Grade - Lot 3016 KXW) was added to give the final desired volume. Additional HCl was added in small aliquots to effect complete dissolution. This solution was pumped through the thermostatted column (25.0 ± 0.1°C), and a polytetrafluoroethylene (PTFE) needle valve on the column outlet was adjusted to give a measured effluent flow rate of 6.0 mL/hr. In all, 245 samples (2 mg calcium per 2-mL sample) were collected over the total elapsed run time of 80.78 hr (target sampling rate = 20 min/sample). Resin bed depth remained at 99.7 ± 0.1 cm throughout the experiment.

To correct for sample size variations caused by evaporation of the methanol, the samples were evaporated to dryness before processing. The samples were reconstituted with the addition of 2.0 mL of deionized H_2O. One-mL aliquots were removed and the calcium concentration measured by flame atomic absorption spectroscopy (air/propane flame, Buck Scientific Co. Model 200 AAS, computerized data acquisition). Preparation of the samples for isotopic ratio measurements is currently in progress.

The calcium breakthrough curve is shown in Figure II-6. Since the cryptand bonds calcium by ion-dipole interactions, the frontal boundary is more diffuse than it would be in an ion exchange system where bonding is of an ion-ion nature. However, even without lithium preloading to sharpen the front, this system still exhibits quite acceptable behavior. The number of theoretical plates in the column was obtained from the gradient of the frontal boundary curve at its inflection point [8]. Under the given experimental conditions, approximately 2,900 stages were realized in the 9.7-cm bed length with a corresponding height equivalent to a theoretical plate (HETP) of 0.34 mm.

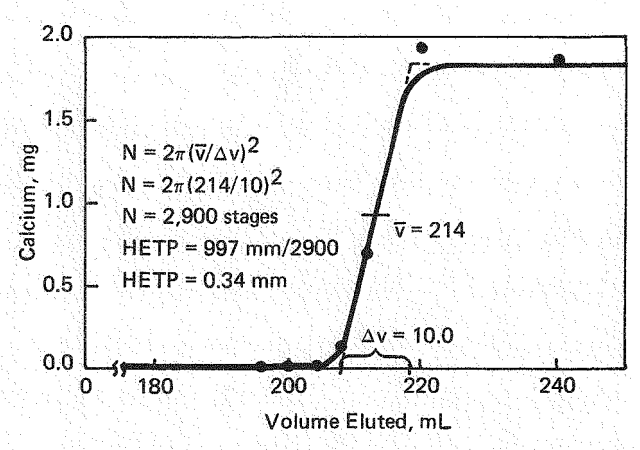

FIGURE II-6 - Calcium breakthrough curve and HETP calculation from 222B cryptand resin column experiment.

Preliminary Results from Previous Column Experiments

Isotopic composition data were received from Oak Ridge National Laboratory for parts of the calcium hydroxide-sulfonic acid resin (10°C) and calcium methyliminodiacetate-sodium sulfonate resin experiments performed previously (Table II-4). These data were obtained during a period of instrument problems and method development and are considered preliminary even though the measurements exhibit acceptable precision.

These results indicate that calcium isotope fractionation occurred in the calcium hydroxide experiment, but did not occur significantly in the calcium methyliminodiacetate column run. The exact separation factor for the calcium hydroxide system cannot be reliably determined from only these preliminary data. The separation factor will be calculated and reported on when additional isotopic ratio data become available. A complete understanding of the observed lack of isotope separation in the calcium methyliminodiacetate system must await results from a previously reported experiment [9] performed to verify the Soviet claim of a large iminodiacetate (IMDA) isotope effect.

BATCH EXPERIMENTS

Liquid-Liquid Chemical Exchange

Research has begun to find effective liquid ion exchange reagents for use in calcium liquid-liquid chemical exchange systems. In the past, di-2-ethylhexylphosphoric acid (DEHPA) has been used in this role in systems designed to take advantage of the known calcium-crown ether isotope effect. However, in addition to functioning as an ion exchanger, DEHPA is also an extractant for calcium. This extraction has a

Table II-4 - CALCIUM COLUMN EXPERIMENT RESULTS

Experiment	Sample No.	At. % 40	42	43	44	48
$Ca(OH)_2$	217	96.865	0.654	0.137	2.145	0.199
	222	96.925	0.647	0.136	2.099	0.193
	224	96.925	0.648	0.137	2.099	0.191
	227	96.930	0.647	0.136	2.097	0.191
	232	96.936	0.645	0.134	2.097	0.188
	243	96.935	0.646	0.135	2.096	0.189
	247	96.936	0.645	0.135	2.094	0.189
	252	96.937	0.647	0.135	2.091	0.189
Calcium Methyliminodiacetate	345	96.936	0.646	0.135	2.093	0.189
(CaMIMDA)	348	96.934	0.647	0.136	2.092	0.192
	350	96.936	0.646	0.136	2.093	0.189
	352	96.929	0.646	0.137	2.092	0.196
	355	96.934	0.646	0.137	2.093	0.191
	360	96.935	0.646	0.135	2.092	0.191
	375	96.934	0.644	0.134	2.091	0.197
	380	96.934	0.644	0.135	2.088	0.199

measured isotope effect that is approximately one-fourth the magnitude of the calcium-crown ether isotope effect. Hence, the observed overall calcium isotope separation measured in systems with both crown ethers and DEHPA may be reduced by an amount proportional to the degree to which the DEHPA effectively competes with the crown ether in complexing calcium.

Exploration of various LIX® reagents* has been started to assess their utility as nonextracting ion exchangers in calcium systems. These reagents are a family of hydroxyoximes with the general structure shown in Figure II-7. Systems investigated to date with several of the LIX® reagents have indicated calcium organic/aqueous distribution coefficients in the range of 0.1 to 0.2. Preliminary results indicate that calcium extraction by the LIX® reagent ranges from negligible to possibly significant, depending on experimental conditions. Optimization of these systems is being performed to increase the calcium distribution ratios before separation factor measurements are conducted.

Other compounds, such as dinonylnaphthalenesulfonic acid, are also being explored as alternative liquid ion exchangers. In the case of an organic sulfonic acid, the goal is to derive a liquid-liquid analog to a liquid-solid system using a sulfonic acid resin as the ion exchanger.

Phase Separator Development

Complete characterization of liquid-liquid chemical exchange isotope separation systems requires a determination of the heterogeneous isotopic exchange rate. This parameter has

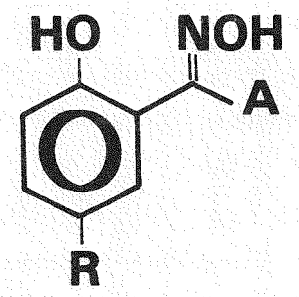

FIGURE II-7 - General structure of hydroxyoximes (LIX reagents). (From: The Chemistry of Metals Recovery Using LIX® Reagents, Henkel Corporation, Minerals Industry Division Red Book, p. 23.)

historically been determined by perturbing the isotopic composition of one phase and monitoring the time required for the system to return to equilibrium. This method requires a means for rapidly and completely separating the system phases so that the isotopic composition of at least one phase can be determined without contamination from the other phase.

A centrifugal phase separator has been effectively used at Mound for these measurements. However, it was complicated to adjust for maximum separation efficiency and was also subject to leakage from the rotating seals utilized. The development of replacement devices is under way to remedy these problems.

A phase separator based on a preferentially wettable membrane was constructed (Figure II-8) by modifying the design employed by Bäckström, et al. [10] for continuous flow extraction. Since this separator has no moving parts and smaller holdup volumes, it should be capable of more reliable performance and shorter residence times than the centrifugal

*LIX is a registered trademark of Henkel Corp.

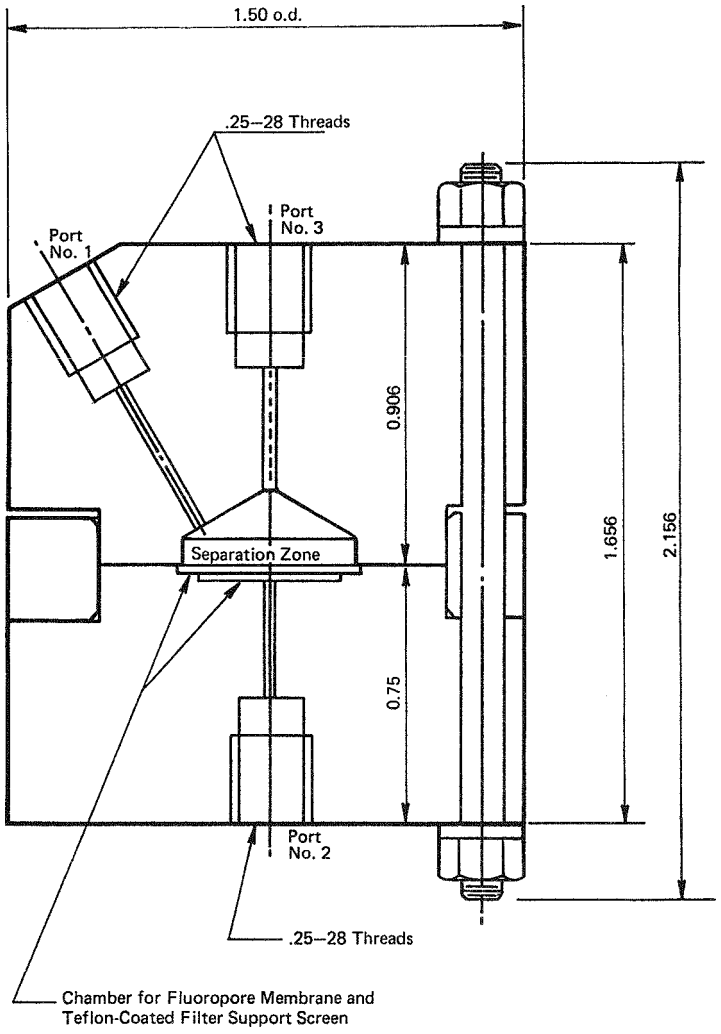

FIGURE II-8 - Teflon membrane phase separator, shown twice its actual size. All dimensions are in inches and represent the actual sizes.

separator. In addition, this type of device can be used for liquid-solid sorption and exchange rate determinations which are not possible with a centrifugal separator designed for liquid-liquid systems. Performance will be determined by membrane characteristics and flow rates used; hence, different membrane materials are currently being evaluated.

In order to be able to measure heterogeneous exchange rates in as wide a range of systems as possible, construction of a new centrifugal phase separator has begun. This device is derived from the previous Mound centrifuge, but will be modified to include a magnetically coupled rotor drive to eliminate rotating seals. This device will be used for those systems that cannot be separated effectively by the membrane separator. Testing and validation will be performed as soon as construction is completed.

III. Calculations in Plutonium Chemistry

Speciation of Plutonium in Environmental Waters

G. L. Silver

Choppin recently published an interesting paper about the fate of plutonium in the environment, a topic of perennial interest [1]. Choppin's paper is likely to be used as a source of information about this contentious subject, so it seems appropriate to point out that his paper raises many questions and may contain some errors. These issues should be clarified by those who use the work as a literature citation.

For example, Choppin provides a list of the logarithms of the stability constants of plutonium oxidation states with various ligands. The list occurs as his Table 3, and it contains entries for the carbonate complexes of tetravalent plutonium. The entries are said to be "the most reasonable available . . ." The question arises: Who sets the standard for reasonableness, and on what basis is reasonableness determined? The formation constants of carbonate complexes is a subject of interest to all environmental scientists. Thus, it is not impertinent to wonder how Choppin's estimates were made and why his numbers are superior to other estimates. Mere say-so does not suffice for so important a subject. Rai and Ryan [2] recently commented that the values of the tetravalent actinide carbonate complexes reported in the literature are grossly in error. Since Choppin provided no justification for his numbers, the reader can assume that Rai and Ryan's conclusion [2] applies to Choppin's entries as fairly as to any others.

Choppin proceeds with the calculation of plutonium species in seawater and freshwater. For this purpose he uses his Equations 1-4. But did he really use these equations as they are presented? The equations do not seem to be dimensionally homogeneous. What appears to be missing in the equations is the Faraday constant, usually abbreviated by the letter F. While the matter is not absolutely clear, this may be an oversight.

Choppin lists the E_h of seawater as 0.8 V, a value he does not justify and that seems higher than values reported elsewhere in the literature of seawater. For example, Aston says the value is 0.729 V [3], while Krauskopf gives a range of values for which the upper limit is 0.3 V [4]. Harvey implies that the potential does not ordinarily fall far from 0.3 V [5], while Hood remarks that it does not usually deviate much from 0.43 V [6]. Richards says that waters near the surface of the Black Sea have potentials close to 0.4 V, but this value diminishes with increasing depth below about 50 m [7]. Garrels and Christ present a diagram in which "normal ocean water" is given a pH of about 8 and an E_h of about 0.4 V [8]. The point is that none of the listed sources give a value as high as that used by Choppin.

The values of E_h for freshwater are calculated next, supposedly by use of Choppin's Equation 5. This equation gives the E_h of freshwater at pH 8 as about 7.5 V, an unusually high value for a freshwater system and much higher than the value for seawater at almost the same pH. It is possible to estimate the

potentials really used by Choppin by applying the Nernst equation to the ratio $[PuO_2^{2+}]/[PuO_2^{+}]$ for each pH value in his Table 4. With these values and the least squares method, his Equation 5 should probably have contained a constant that is approximately 0.8 and a pH coefficient that is approximately -0.06.

Choppin proceeds by listing some ligands that occur in seawater as well as freshwater. This is followed by calculating the ratio $[Pu(IV)Hu]/[PuO_2^{2+}]$ from his Equations 7-9. These equations are a mixture of unbalanced whole reactions and unbalanced half reactions. Incorrect values of the desired ratio appear to have resulted from improper use of this blend. Consider the case of freshwater at pH 6 and zero ionic strength. The Nernst equation for the system, as applied to "free" ions of hexavalent and pentavalent plutonium (see his Table 4), yields

$$E = 0.96 + 0.05916 \log(2.27 \times 10^{-9}) \quad (1)$$

or E = 0.4486 V for freshwater at pH 6. The logarithm of the formation constant for the first humate complex of tetravalent plutonium is given as 17.5. Other complexes do not seem to be important and are not considered by Choppin. Thus, the alpha coefficient for tetravalent plutonium is:

$$AX = ([Pu^{4+}] + [Pu(IV)Hu])/[Pu^{4+}] \quad (2a)$$

$$AX = ([Pu^{4+}] + [Pu^{4+}](10^{17.5})(10^{-5.5})/[Pu^{4+}] \quad (2b)$$

or

$$AX = 1 + 10^{12} = 10^{12}.$$

In this calculation, it is to be remembered that an alpha coefficient is the ratio of the total concentration of the soluble oxidation state to the "free" or uncomplexed concentration of the same oxidation state. (It should also be noted that the species $PuOH^{3+}$ has been neglected for the sake of simplicity. The alpha coefficient for the reaction between Pu^{4+} and the hydroxide ion is small compared to the alpha coefficient for reaction between humic acid and Pu^{4+}, so little error is introduced by this omission.) Rewriting the ratio yields

$$[Pu(IV)_{total}] = (AX)([Pu^{4+}]). \quad (2c)$$

The Nernst equation may now be applied to the hexavalent/tetravalent couple in freshwater at pH 6 and zero ionic strength:

$$E = 1.032 + 0.02958 \log([PuO_2^{2+}][H^4]/[Pu^{4+}]) \quad (3)$$

However, the term $[Pu^{4+}]$ can be removed from Equation (3), and the term $[Pu(IV)_{total}]$ can be introduced by substitution from Equation (2c). This is useful because the terms $[Pu(IV)_{total}]$ and [Pu(IV)Hu] are practically equal. In other words, the complexation of tetravalent plutonium by humic acid is so complete that for practical purposes the total concentration of tetravalent plutonium is the same as the concentration of the 1:1 tetravalent plutonium-humic acid complex. The substitution being made, the argument of the logarithm in Equation (3) becomes a ratio whose numerator is the product of the alpha coefficient AX, the fourth power of the hydrogen ion concentration, and the concentration of uncomplexed, "free"

hexavalent plutonium. The denominator of the ratio is the total concentration of tetravalent plutonium, or, to a high degree of accuracy, the concentration of the Pu(IV) humate complex. Solving for the ratio $[Pu(IV)Hu]/[PuO_2^{2+}]$ produces a number which is about $(5)(10^7)$, a number which differs substantially from the 10^{23} obtained by Choppin.

A first check on the accuracy of these calculations can be obtained by a calculator program presented several years ago [9]. The following data about freshwater at pH 6 can be obtained from Choppin's Table 4, while their interpretations are explained in Reference 10. K1 = 0.0298, K2 = 7.03, AW = AY = AZ = 1 (no complexation of trivalent, pentavalent, and hexavalent plutonium; their alpha coefficients are unity), potential of freshwater in question = 0.4486 V, and acidity = 10^{-6} M. From Choppin's Table 2, the standard potential of the appropriate [VI]/[V] couple is 0.96 V. The alpha coefficient for tetravalent plutonium (AX), considering only the 1:1 humate complex as Choppin does in his Equations 7-9, is 10^{12}. Substitution of these numbers into the calculator program yields the plutonium oxidation state distribution. The value of the ratio under discussion is again found to be about $(5)(10^7)$, which is in agreement with the more cumbersome method described above.

The foregoing calculations are tedious, and for that reason mistakes are easily made. Even the process of entering the data into HP-67 or HP-97 calculators can result in blunders, so the author does not offer this result as beyond criticism. The reader should check it to satisfy himself. The point is that results such as those presented by Choppin or anyone else are more in need of critical inspection than they are in need of uncritical acceptance. Choppin's paper, and this author's questions, illustrate that even 40 yr after the discovery of plutonium there is still no agreement on how to perform equilibrium calculations. This represents a problem as significant and important as any now faced in the field.

In his Table 6, Choppin presents the distribution of species of hexavalent plutonium. At pH 6, the species are entirely the hydroxide complexes. The concentration of a 1:1 metal-ligand complex in solution is related to the product of the concentration of the ligand and the applicable formation constant. The larger this product for a specified metal ion concentration, the larger the concentration of the complex is. For simplicity, consider only the concentrations of the 1:1 hydroxide and 1:1 humate complexes. For hexavalent plutonium, the product of the hydroxide ion concentration and the appropriate formation constant appears to be $(10^{-8})(10^{8.4})$, while the product of the humate concentration and the appropriate formation constant appears to be $(10^{-5.5})(10^7)$. Thus, there is reason to suspect that at pH 6 the 1:1 humate complex is more important than the 1:1 hydroxide complex because its respective product is larger. Choppin's Table 6 does not reflect this.

Why does Choppin's Table 6 exclude humate complexes? Is it because "all" the hexavalent plutonium is supposed to be reduced by humic acid? The reactions of

complexation and reduction are not mutually exclusive; they are parallel, and they influence one another. Even if most of the hexavalent plutonium is reduced by humic acid, what remains will be divided among all possible complexes, including complexes with the reducing agent if such complexes can form. Complexation with the reducing agent is not reflected in Choppin's Table 6, but it deserves to be mentioned.

In his Table 7, Choppin lists a nonequilibrium distribution of plutonium ions established through reduction of the hexavalent state by humic acid. He also lists the equilibrium distribution established after reduction. The fraction of hexavalent plutonium in freshwater at pH 6 is about 10^{-34} in the nonequilibrium case. Since hexavalent plutonium is thought to be complexed at pH 6, whereas pentavalent plutonium remains uncomplexed, the ratio of the "free" ions $[PuO_2^{2+}]/[PuO_2^{+}]$ in the nonequilibrium case must be less than 10^{-31}. This corresponds to a potential of less than -0.85 V, a potential that lies below the lowest potentials ordinarily observed in natural waters. It would be interesting to know something about the biological system that can induce such potentials and remain in this nonequilibrium condition.

The entries in Choppin's Table 7 for equilibrium in seawater after reduction of PuO_2^{2+} are interesting. Here, the mole fraction of hexavalent plutonium in seawater is said to be unity after it has been reduced. The total concentration of plutonium in seawater is about 10^{-17} M and the concentration of humate is about 10^{-7} M according to Choppin's tables. Thus, the concentration of the reducing agent exceeds the total plutonium concentration by a factor of about 10^{10}. If a small portion of the humic acid can initially reduce nearly all the hexavalent plutonium, why can't another small portion reduce any plutonium which somehow gets reoxidized to the hexavalent state? Why doesn't the substantial excess of humic acid keep the hexavalent state reduced once the tendency to reduction has been established? Why is humic a reducing agent on one occasion, but inert on subsequent occasions?

These are the kinds of questions and uncertainties raised by Choppin's contribution. Their resolution should aid in understanding his paper and perhaps in understanding the chemistry of plutonium in the environment. Choppin remarks that his observations support either a nonequilibrium model or a lower E_h for an unspecified plutonium half-cell. It may occur to the reader that what is put into question is the E_h of seawater, not just the E_h values of plutonium half-cells. After examining many contingencies, Choppin concludes that "the system could . . . reestablish equilibrium . . . or remain in the nonequilibrium condition," a conclusion unlikely to generate controversy because there are no other possibilities.

Although it may only be a matter of semantics, it might be preferable to say "a nonequilibrium condition" rather than "the nonequilibrium condition." There is only one equilibrium composition for a plutonium system, but an infinite number of nonequilibrium compositions exist. A nonequilibrium state should be characterized as carefully as the equilibrium state, for the reader is entitled to know why one nonequilibrium state is preferred above all others.

References

I. Low Temperature Research

1. Berry, K. H., Metrologia, 15, 89 (1979).

2. Aziz, R. A., V. P. S. Nain, J. S. Carley, W. L. Taylor, and G. T. McConville, J. Chem. Phys., 70, 4330 (1979).

3. McConville, G. T., Proc. 17th Int. Conf. Low Temp. Phys. (North Holland, Amsterdam, 1984), pp. 401-402.

4. Mound Activities in Chemical and Physical Research: July-December 1983, MLM-3150, Monsanto Research Corporation (June 1984), pp. 7-9.

5. Mound Activities in Chemical and Physical Research: January-June 1984, MLM-3195, Monsanto Research Corporation (October 1984), pp. 10-14.

6. Feltgen, R., H. Kirst, K. A. Kohler, H. Panly, F. Torello, J. Chem. Phys., 76, 2360 (1982).

7. Feltgen, R., (private communication, 1984).

8. Steur, P. P. M., M. Durieux, and G. T. McConville (to be published in Metrologia).

9. Gugan, D., Temperature, Its Measurement and Control in Science and Industry, Vol. 5, J. F. Schooley, (ed.), p. 55, Am. Inst. Phys., New York, 1982.

10. Kemp, R. C., L. M. Besley, and W. R. G. Kemp, Temperature, Its Measurement and Control in Science and Industry, Vol. 5, J. F. Schooley, (ed.), p. 33, Am. Inst. Phys., New York, 1982.

11. Kemp, R. C., W. R. G. Kemp, and L. M. Besley (to be published in Metrologia).

12. Guildner, L. A., and R. E. Edsinger, J. Res. NBS, A80, 703 (1976).

13. Aziz, R. A., (private communication, 1986).

14. Ahlrichs, R., R. Penco, and G. Scoles, Chem. Phys. 19, 119 (1970).

15. Hirschfelder, J. O., C. F. Curtiss, and R. B. Bird, Molecular Theory of Gases and Liquids, p. 409, John W. Tey and Sons, 1966.

16. Matacotta, F. C., G. T. McConville, P. P. M. Steur, and M. Durieux (to be published in Metrologia).

17. Cameron, J. A., and G. M. Seidel, J. Chem. Phys., 83, 3621 (1985).

18. Keller, W. E., Phys. Rev., 98, 1571 (1955).

19. Roberts, R. T., R. H. Sherman, and S. G. Sydoriak, J. Res. NBS, 68A, 567 (1964).

II. Separation Research

1. Rutherford, W. M., J. Chem. Phys., 81, 6136 (1984).

2. Mound Activities in Chemical and Physical Research: January-June 1985, MLM-3305, Monsanto Research Corporation (October 1985), p. 5.

3. Ma, N. R., and A. L. Beyerlein, J. Chem. Phys., 78, 7010 (1983).

4. Mound Activities in Chemical and Physical Research: July-December 1984, MLM-3258, Monsanto Research Corporation (June 1985), p. 10.

5. Mound Activities in Chemical and Physical Research: July-December 1985, MLM-3347, Monsanto Research Corporation (April 1986), p. 27.

6. de la Garza, A., Chem. Engr. Science, 18, 73 (1963).

7. Heumann, K. G., and H. P. Schiefer, Angew. Chem., 92, 406 (1980).

8. Separation of Isotopes, H. London, ed., George Newnes Limited Publishing, 1961, pp. 230-233.

9. Mound Activities in Chemical and Physical Research: January-June 1986, MLM-3389, Monsanto Research Corporation (October 1986), p. 8.

10. Bäckström, K., Lars-Göran Danielsson, and Lage Nord, "Design and Evaluation of a New Phase Separator for Liquid-Liquid Extraction in Flow Systems," Analytica Chimica Acta, 169 (1985), 43-9.

III. Calculations in Plutonium Chemistry

1. Choppin, G. R., in Environmental Inorganic Chemistry, a series of papers presented at the U. S.-Italy Joint Seminar and Workshop on Environmental Inorganic Chemistry, 1983, pp. 307-320 (1985), K. Irgolic and A. Martell (eds.). Chemical Abstracts, 104, 155429m (1986).

2. Rai, D., and J. L. Ryan, Inorg. Chem., 24:3, 247 (1985).

3. Aston, S. R., Mar. Chem., 8, 319, (1980).

4. Krauskopf, K. B., Introduction to Geochemistry, Graw-Hill Book Co., New York, NY, 1967, p. 243.

5. Harvey, H. W., The Chemistry and Fertility of Sea Waters, Cambridge University Press, 1966, p. 152.

6. Hood, D. W., in The Encyclopedia of Oceanography, R. W. Fairbridge (ed.), Reinhold Publishing Corp., New York, NY, 1966, p. 798.

7. Richards, F. A., in Chemical Oceanography, J. P. Riley and G. Skirrow (eds.), Academic Press, New York, NY, 1965, p. 635.

8. Garrels, R. M., and C. L. Christ, Solutions, Minerals, and Equilibria, Freeman, Cooper & Co., San Francisco, CA, 1965, p. 381.

9. Silver, G. L., in Mound Facility Activities in Chemical and Physical Research: July-December 1979, MLM-2727, Monsanto Research Corporation, Miamisburg, Ohio (1980), p. 47.

10. Silver, G. L., Mar. Chem., 12, 91 (1983).

Distribution

EXTERNAL

TIC, UC-4 and UC-22 (260)

H. L. Adair, Oak Ridge National Laboratory

J. R. Blair, DOE/Office of Health and Environmental Research

J. Burnett, DOE/Office of Basic Energy Sciences

J. S. Cantrell, Miami University, Oxford, Ohio

G. R. Gartrell, DOE/Dayton Area Office

K. Gschneidner, Iowa State University of Science and Technology, Ames, Iowa

N. Haberman, DOE/Division of Nuclear Energy

J. N. Maddox, DOE/Office of Health and Environmental Research

J. A. Morley, DOE/Dayton Area Office

L. R. Morss, Argonne National Laboratory

H. A. Schneiderman, Monsanto, St. Louis

F. D. Stevenson, DOE/Office of Basic Energy Sciences

L. Thompson, University of Minnesota

E. L. Venturini, Sandia National Laboratories, Albuquerque

D. White, University of Pennsylvania

Monsanto Reports Library, R2C, St. Louis

INTERNAL

G. C. Abell

C. T. Bishop

D. Cain

D. G. Carfagno

V. R. Casella

R. E. Ellefson

W. F. Evans

C. S. Friedman

W. B. Hogeman

C. W. Huntington

B. E. Jepson

G. T. McConville

D. A. Menke

E. D. Michaels

R. H. Nimitz

W. K. Park

W. M. Rutherford

P. W. Seabaugh

W. E. Sheehan

G. C. Shockey

G. L. Silver

W. L. Taylor

R. J. Tomasoski

C. J. Wiedenheft

W. R. Wilkes

H. A. Woltermann

R. W. York

Document Control

Library (15)

Publications

Technical Publications
Lisa R. Kramer, Editor